

INTERNATIONAL SOCIETY FOR SOIL MECHANICS AND GEOTECHNICAL ENGINEERING



This paper was downloaded from the Online Library of the International Society for Soil Mechanics and Geotechnical Engineering (ISSMGE). The library is available here:

<https://www.issmge.org/publications/online-library>

This is an open-access database that archives thousands of papers published under the Auspices of the ISSMGE and maintained by the Innovation and Development Committee of ISSMGE.

The paper was published in the proceedings of the 7th International Young Geotechnical Engineers Conference and was edited by Brendan Scott. The conference was held from April 29th to May 1st 2022 in Sydney, Australia.

A review of the hydro-mechanical behaviour of tailings and its importance to the stability of tailings dams

Une révision du comportement hydromécanique des rejets et son importance pour la stabilité des parcs à rejets.

Camilo Morales & David Taborda

Civil and Environmental Engineering, Imperial College London, United Kingdom

Camilo Morales

SRK Consulting, camorales@srk.cl

ABSTRACT: Seepage in tailings storage facilities (TSFs) is commonly assumed to occur under gravity flow and is usually determined for steady-state conditions. However, the stability of TSFs is highly influenced by the degree of saturation of the materials involved in these structures. Several of these structures are in areas where the climate conditions are characterised by alternating (very) dry and (very) wet seasons, which presents additional challenges in terms of soil-atmosphere interaction. This paper presents a review of the parameters that influence the phreatic surface within the TSF under steady-state conditions and assesses by a numerical analysis of how this behaviour changes under transient conditions. For the modelling stage, a generic upstream dam setting is analysed using the limit equilibrium approach, where steady-state and transient seepage analyses are employed to assess the most influencing parameters on the dam's stability. Specifically, the hydraulic boundary conditions, the length, anisotropy and uniformity of the beach, and the effect of considering the drying or wetting path of the soil-water characteristic curve, are assessed to determine the degree of influence of these parameters on the stability of the dam.

RÉSUMÉ : L'infiltration dans les sites d'entreposage de rejets miniers se produit, généralement, sous l'effet de la gravité et on la détermine habituellement pour des conditions de flux stables. Cependant, la stabilité des parcs à rejets est fortement influencée par le degré de saturation des matériaux impliqués dans ces structures. Plusieurs de ces structures se trouvent dans des zones où les conditions climatiques sont caractérisées par une alternance de saisons (très) sèches et (très) humides, ce qui présente des défis supplémentaires, en termes d'interaction sol-atmosphère. Cet article présente une révision des paramètres qui influencent le niveau phréatique dans un parc à rejets, en régime permanent, et évalue par une analyse numérique, comment ce comportement change pour des conditions transitoires. Pour l'étape de modélisation, un barrage amont typique est analysé en utilisant l'approche de l'équilibre limite, où des analyses d'infiltration en régime permanent et transitoire sont utilisées pour évaluer les paramètres les plus influents sur la stabilité du parc à rejets. Plus précisément, les conditions hydrauliques limites, la longueur, l'anisotropie et l'uniformité de la plage, et l'effet de la prise en compte du chemin de séchage ou de mouillage de la courbe de rétention d'eau, sont évalués pour déterminer le degré d'influence de ces paramètres sur la stabilité du parc à rejets.

KEYWORDS: upstream tailings dams stability, seepage analysis, limit equilibrium analysis, unsaturated soil mechanics, mine waste management.

1 INTRODUCTION

Mine tailings are the leading waste produced due to mining exploitation. They include the chemicals used to extract the ore, uneconomic metals, minerals, organisms and usually a significant amount of water (Heidarian, 2012). With the increased demand for commodities, finding ore bodies with a high mining grade is increasingly tricky (Blight, 2010). Even with high mining grades, from 100 tons of rock, around 99% will end as mining waste that must be stored somewhere.

Several tailings dams failures have been reported in the literature in the second part of the 20th century (Rico et al. 2008). In particular, in the last decade, particular interest has arisen the catastrophic dam disasters that occurred in Mount Polley in Canada in 2014 and the failures of the Brazilian dams in the Fundão dam in 2015 and more recently in the Feijão I dam in 2019. All of them causing severe environmental damages (Morgenstern et al., 2015; Morgenstern et al. 2016; Robertson et al. 2019).

Rico et al. (2008) and Saad (2008) established that the main reasons for failure in tailings dams are issues related to water management. Most of the failures occur in upstream tailings dam facilities (UTSFs), being the most critical triggers: static liquefaction, extreme rainfall scenarios, piping, and overtopping of the beach, respectively. These factors are either directly or indirectly related to saturated soil undergoing high pore-water

pressures, hydraulic gradients, or a high phreatic surface (Brisson 2006).

Since extreme weather events such as severe rainfalls and droughts are becoming more common in part, favoured by global warming (O'Gorman, 2015). It is necessary to understand the hydro-mechanical behaviour of tailings and the main factors affecting the stability of tailings storage facilities (TSFs) in both steady-state and transient behaviours. Analysing this kind of problems is essentially a partially saturated soil mechanics issue since tailings dams are usually subjected to continuous cycles of drying (evaporation and evapotranspiration) and wetting (precipitation and the continuous process of spigot disposal).

In this context, the soil-water characteristic curve (SWCC) has proven to be an essential tool to understand how the water content varies at different soil suction levels indicating the free energy state of the soil water. In a few words, the SWCC shows how the water and air interact with the solid particles for different degrees of saturation, being crucial to understanding unsaturated soil behaviour (Fredlund & Xing, 1994; Ng & Menzies, 2007; Malaya & Sreedeeep, 2012). The SWCC is a helpful tool for numerical modelling since many engineering properties can be obtained from the SWCC, such as hydraulic conductivity, shear strength and thermal conductivity, among others (Fredlund & Rahardjo, 1993).

This research focuses on the unsaturated flow through tailings slimes and how this can influence the overall stability of a

generic upstream sand dam that stores slimes in its impoundment.

Little significance is given to the unsaturated shear strength properties due to the lack of experimental data regarding how the shear strength varies with increasing suction for tailings. Several factors are studied to determine their importance in the stability of UTSFs for steady-state and transient analyses, including the pond's location from the crest of the dam (beach length), drainage system efficiency, and the hydraulic properties of the dam tailings slimes and sands.

2 DATA CALIBRATION

2.1 Gravimetric water content-SWCC

The SWCC can be expressed in terms of gravimetric water content (w), volumetric water content (θ_w), or the degree of saturation (S_r) versus suction. In geotechnical engineering practice, the SWCC is usually measured as the gravimetric water content existing for a certain amount of soil suction since it is easier to measure it in that way in the laboratory. In this context, the gravimetric water content can be expressed as Eq. 1 shows:

$$\theta_w = S_r \frac{e}{1+e} = w \frac{\rho_d}{\rho_w} = w \frac{G_s}{1+e} \quad (1)$$

Where e , ρ_d , ρ_w and G_s are the void ratio, soil's dry density, water density and specific gravity of the soil, respectively. Figure 1 shows an example of copper and iron sand tailings and slimes grouped by bands that show different types of behaviour (Musso and Suazo 2019, Robertson et al. 2019).

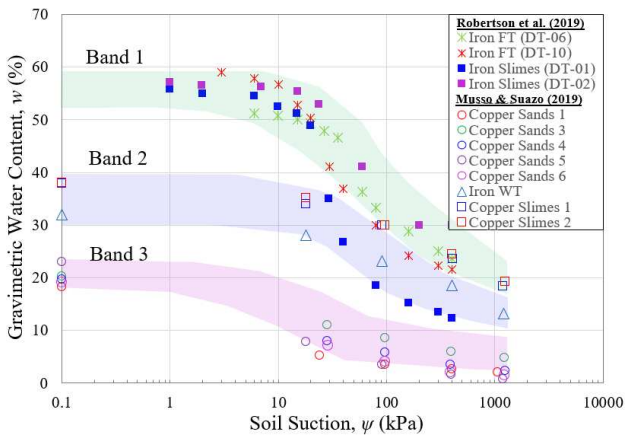


Figure 1. Bands defined for tailings, sands and slimes.

From Figure 1, the finer the tailings are (e.g., slimes or fine tailings), the more water it can retain, especially at very low suctions, representing nearly a 100% saturated state of the soil. Another important detail is that fine tailings (FT) or iron slimes can hold even more water than fine copper tailings. The same occurs with copper tailings sands that are less capable of retaining water than iron whole tailings (WT).

To use these tests in computational models, the results presented in Figure 1 were adjusted by some of the SWCC fitting equations available in the literature. Specifically, the van Genuchten (1980) and Fredlund and Xing (1994) equations were used. These models are presented in Eq. (2) and (3), respectively.

$$w(\psi) = w_r + (w_{sat} - w_r) \left(\frac{1}{1 + (a_{vg}\psi)^{n_{vg}}} \right)^{m_{vg}} \quad (2)$$

$$w(\psi) = C(\psi) \frac{w_{sat}}{(e + (\psi/a_f)^{n_f})^{m_f}} \quad (3)$$

Where $C(\psi)$ is defined as a correction factor that transforms Fredlund and Xing equation in a 4-parameter (a_f, n_f, m_f, h_r) continuous equation valid up to 10^6 kPa, i.e. until completely dry conditions, as Eq. 4 shows:

$$C(\psi) = 1 - \frac{\ln(1 + \frac{\psi}{h_r})}{\ln(1 + \frac{10^6}{h_r})} \quad (4)$$

Zhai & Rahardjo (2021) defined the Fredlund & Xing (1994) equation as "Method A" when the correction factor $C(\psi)$ is used, and Fredlund & Xing method B when $C(\psi)=1.0$ is considered. Figure 2 presents the average square error obtained by the data fitting of each equation. From the results, van Genuchten produces more error with fine-grained soils (slimes and fine tailings) and better results with coarser soils (sands). In general terms, Fredlund & Xing (1994) produces consistently good results for all the types of tailings analysed. In terms of the differences between method A and B, the results obtained by method A tends to be slightly better for sandy soils and almost the same that those obtained by method B for finer soils.

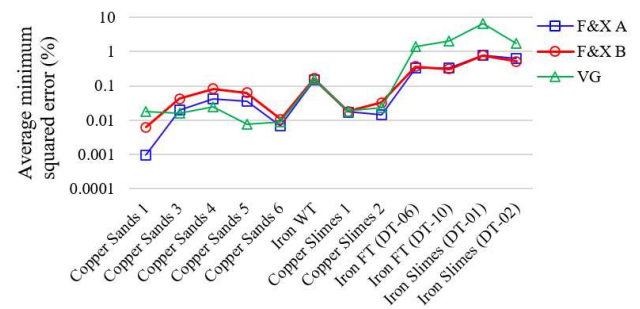


Figure 2. Fitting of van Genuchten (1980) and Fredlund & Xing (1994) equations for Copper Sands of Musso and Suazo (2019).

2.2 Shrinkage Curve and Volumetric water content-SWCC

Although it is very common to obtain the SWCC in terms of the gravimetric water content, most of the statistical models used to obtain the permeability function from the SWCC uses the volumetric water content versus soil suction curve (Leong and Rahardjo 1997). From Eq. 1, it is known that the water content depends on the void ratio. This relationship can be obtained by the Shrinkage Curve. However, it is rare to find sufficient data in the literature from the Shrinkage Curve of tailings.

Figure 3 presents the results of shrinkage curves tests performed in copper tailings (Qiu and Sego 2001) and gold tailings (Heidarian 2012).

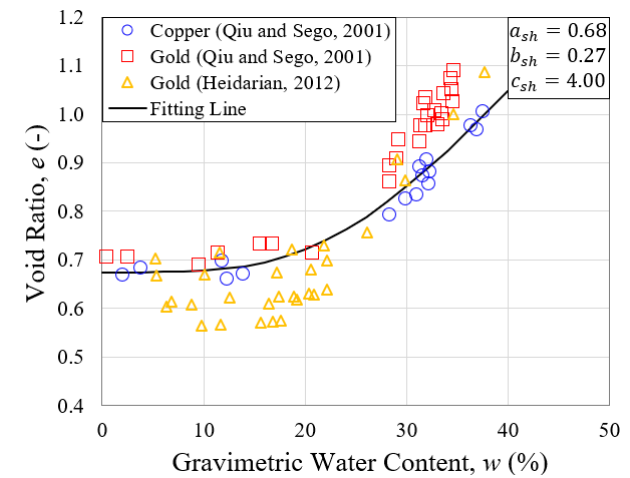


Figure 3. Shrinkage curve for different tailings slimes and the best fit obtained for copper tailings slimes.

The values shown in the upper right corner of Figure 3 among the fitting curve obtained are based on the expression proposed by Fredlund, Wilson & Fredlund (2002) presented in Eq. 5:

$$e(w) = a_{sh} \left(\left(\frac{w}{b_{sh}} \right)^{c_{sh}} + 1 \right)^{1/c_{sh}} \quad (5)$$

This curve represents the relationship used to obtain the volumetric water content SWCC for the statistical model to assess the vertical permeability. In terms of the tailings sands, they are commonly compacted up to 95% of the modified proctor for dam construction. Therefore, no significant volumetric change ($\Delta e=0$) can be assumed in this material, i.e. the void ratio can be assumed constant. Based on this, Figure 4 presents some of the tests reported in Figure 1 in terms of the volumetric water content and the best fit according to method B of Fredlund & Xing (1994) equation for each test. In addition, Figure 4 shows an average SWCC for the copper slimes and tailings sands by using the Fredlund & Xing (1994) method B equation.

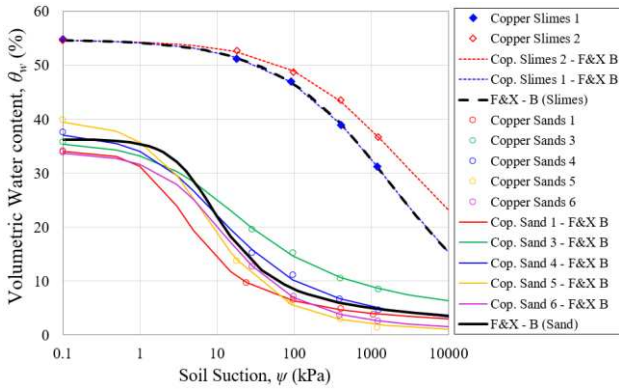


Figure 4. Volumetric SWCC considered for tailings sands and slimes.

Regarding the slimes, the average curve has been adopted as the SWCC fitting of copper slimes 1 of Musso & Suazo (2019) since these are the only pure copper slimes samples available (copper slimes 2 has some content of silver, while tailings from Robertson et al. (2019) correspond to iron tailings that are not considered for the geotechnical model.

2.3 Drying and wetting paths of the SWCC

An important aspect that is usually not considered in unsaturated soil mechanics is the hysteresis of the SWCC. The wetting SWCC is hard to obtain in the laboratory and excessively time-consuming. Fredlund, Rahardjo and Fredlund (2012) suggested that the distance between both curves in the desaturation zone (between the AEV and the residual water content) fluctuates from 0.15 to 0.35 log-cycle, with an average value of 0.25 for sandy soils. While, for silty soils, this value ranges between 0.30 and 0.60, with an average value of 0.5 for well-graded silts.

Based on this recommendation, a horizontal translation of 25% and 50% of a log cycle has been adopted for tailings sands and the slimes, respectively. In the soil suction range, close to saturation (zero soil suction) it has been adopted a reduction of 5% in the saturated volumetric water content for the slimes to consider the irrecoverable volume change produced by drying. While in the sands, this has not been considered since a rigid behaviour of tailings sands was assumed given their dense state due to compaction. Figure 5 presents the drying and wetting SWCCs obtained for tailings sands and slimes.

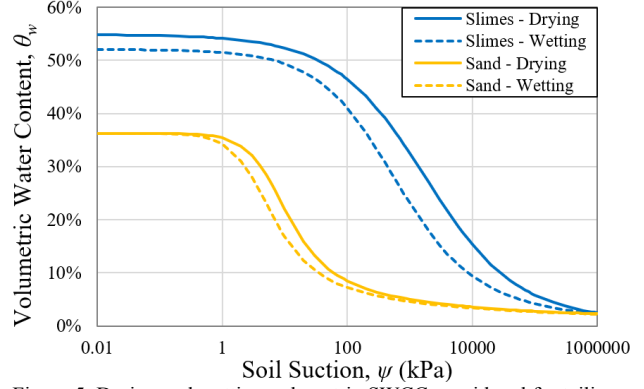


Figure 5. Drying and wetting volumetric SWCC considered for tailings, sands, and slimes.

2.4 Permeability function

It has been proven that the three most influencing parameters are the viscosity of the fluid, the presence of discontinuities and the void ratio (size and shape of soil particles, density, and structure). For homogeneous granular materials, discontinuities are usually neglected as well as changes in the viscosity of the fluid (temperature changes tend to be not significant). For this reason and simplicity in numerical modelling, saturated soils can only be represented as a void ratio function (Leong and Rahardjo 1997). Based on this, Figure 6 shows a set of saturated vertical permeability test results of copper tailings samples with a different amount of fine content (FC).

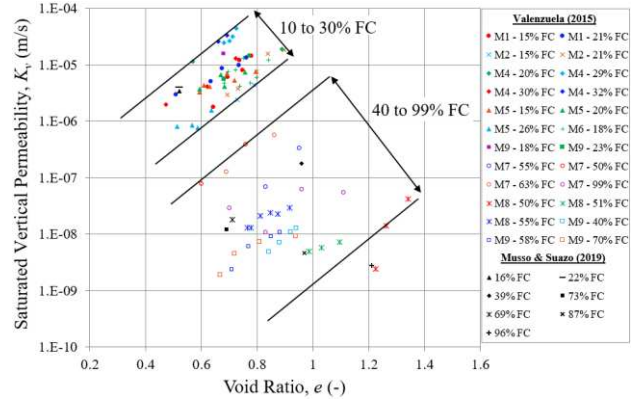


Figure 6. Vertical saturated hydraulic conductivity for different tailings sands and slimes as a function of the void ratio and fines content (after Valenzuela, 2015)

The permeability function has been obtained using the statistical model proposed by Fredlund et al. (1994) presented in Eq. 6. In this expression, the integration limits are ψ_r and ψ_{aev} that represent the residual suction and air-entry values, respectively. On the other hand, $\theta'_w(y)$ is the derivative of the θ_w -SWCC in terms of volumetric water content along with suction, represented by the dummy variable y .

$$k_w(\psi) = k_{sat} \frac{\int_{\psi_r}^{\psi} \frac{\theta_w(y) - \theta_w(\psi)}{y^2} \theta'_w(y) dy}{\int_{\psi_{aev}}^{\psi_r} \frac{\theta_w(y) - \theta_{sat}}{y} \theta'_w(y) dy} \quad (6)$$

To compute the vertical permeability, a code was implemented in Python to integrate the discrete form of Eq. 6 numerically. The results of the saturated coefficients of permeabilities were obtained in Figure 6, and the volumetric water content SWCCs presented in Figure 5 were considered.

Specifically, for the sands, it was considered a k_v^{sat} of $3 \cdot 10^{-6}$ m/s, which is in the average range for void ratios of 0.6 to 0.8 (Sarsby 2013) that can be expected for the sand dam (see Figure

6). For the slimes, two scenarios were considered, coarser slimes (close to the discharge points) and fine slimes (near the pond). For the coarser slimes, it was considered a saturated vertical permeability of $k_v^{sat} = 1 \cdot 10^{-7} \text{ m/s}$ and for fine slimes a $k_v^{sat} = 1 \cdot 10^{-8} \text{ m/s}$, which are in the average and upper zone of the permeability band defined by Valenzuela (2015) for this type of material, respectively (see Figure 6). This differentiation has been adopted considering that segregation usually occurs when tailings are deposited by the subaerial technique in a hydraulic way (spigots, usually located on the crest). Based on this, the computed permeability functions are presented in Figure 7.

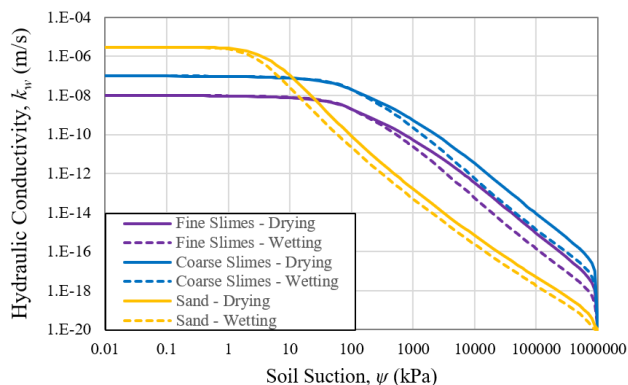


Figure 7. Unsaturated permeability function for tailings sands and slimes for wetting and drying paths.

3 GEOTECHNICAL MODEL

3.1 Geometry

Figure 8 shows the generic model generated used to simulate an upstream dam. Based on this, six geotechnical units can be identified: the foundation soil, basal drain, starter dam, tailings sand dykes rises, coarse slime and fine slimes. The differentiation between coarse slimes and fine slimes lies just in the hydraulic properties to the effect of tailings segregation (usually called "transition zone"). In general terms, the dam has 50 m height with a start dam of 10 m height and sand dyke rises of 5 m. The overall downstream slope of the dam is 4:1 (H:V), while the sand dykes have an overall slope of 3:1 (H:V).

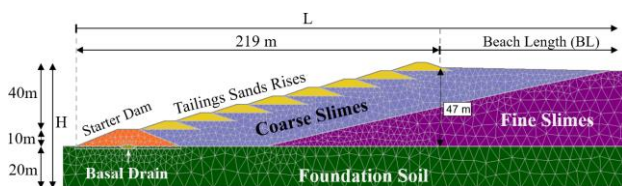


Figure 8. Unsaturated permeability function for tailings sands and slimes for wetting and drying paths.

3.2 Material properties

Table 1 presents the saturated permeabilities in the vertical and horizontal directions for the steady-state analysis. According to Table 1, foundation soil is excluded because it is considered as an impervious boundary for simplicity.

Table 1. Saturated permeability considered for tailings.

Material	$k_v^{sat} \text{ (m/s)}$	$k_h^{sat} \text{ (m/s)}$
Tailings Sands	$3 \cdot 10^{-6}$	$1.5 \cdot 10^{-5}$
Coarse Slimes	$1 \cdot 10^{-7}$	$1 \cdot 10^{-6}$
Fine Slimes	$1 \cdot 10^{-8}$	$1 \cdot 10^{-7}$

Regarding the anisotropy of tailings, an increase of 10 and 5 times in the horizontal direction has been considered for the slimes and tailings sands, respectively. These values follow similar procedures available in the literature for steady-state analyses, such as Valenzuela (2015) and Sarsby (2013). Regarding coarser materials, a saturated constant permeability of $k_v^{sat} = 1 \cdot 10^{-5} \text{ m/s}$ and $k_h^{sat} = 1 \cdot 10^{-4} \text{ m/s}$ (for both directions) has been considered for the starter dam and drainage system, respectively (Blight 2010; Kulhawy and Mayne 1990). For the transient analysis, the permeability for tailings is computed in Figure 7.

In terms of the mechanical properties, Table 2 presents the Mohr-Coulomb parameters adopted for each unit. Again, to isolate the effect of the foundation, this has been considered for simplicity with infinite strength. In general terms, tailings slimes and sands were considered cohesionless according to Blight (2010) and Sarsby (2013). In terms of the friction angle, this was considered using the average parameters provided by Vick (1983). Finally, coarse materials such as the drain and the starter dam were considered using Kulhawy and Mayne (1990) for medium dense gravel.

Table 2. Mohr-Coulomb parameters adopted for each geotechnical unit.

Material	$\gamma_d \left(\frac{kN}{m^3} \right)$	$c' \text{ (kPa)}$	$\phi' \text{ (}^\circ\text{)}$
Drain/Starter dam	20.0	0	38
Tailings Sands	16.0	0	35
Slimes	13.6	0	20

Since an increase in suctions causes an increase in the contact forces between the soil particles, suction can be expected to cause a gain in shear strength. Fredlund, Morgenstern & Widger (1978) extended the Mohr-Coulomb failure criterion for partially saturated soil mechanics incorporating this effect. According to this, Eq. 6 presents the bi-linear expression suggested:

$$\tau = c' + (\sigma - u_a) \tan \phi' + (u_a - u_w) \tan \phi^b \quad (6)$$

Where u_a is the pore-air pressure, $(\sigma - u_a)$ is the net stress normal to the failure shearing plane and ϕ^b is the friction angle relative to soil suction. Based on this, for simplicity, in this research ϕ^b is considered equal to the angle of friction (ϕ'), under the assumption of low suctions in the unsaturated zone.

3.3 Modelling considerations

The geotechnical model was discretised by 3,502 3-nodes triangular elements with an average element size of 2 m close to the dam. Based on this, a steady-state analysis considering a base case scenario with a beach length of 50 m and the basal drain working appropriately (zero pressure boundary condition) was analysed to establish the phreatic surface. For the analysis, the hydraulic properties presented in Table 1 and the permeability functions presented in Figure 7 for the wetting path were considered.

Once the phreatic surface has been established by the steady-state analysis, transient analysis is computed considering a rainy season of the Amazonas (Climate-Data.org., n.d.) simulated by 16 weeks of heavy rainfall and then four weeks of dry conditions, as Figure 9 shows. After each of these analyses, the Factor of Safety (FoS) is calculated with a limit equilibrium analysis (LEA) considering the Spencer (1967) methodology to assess the influence of the beach length, drain condition (clogged or fully operative), segregation of tailings (uniform slimes beach), anisotropy of slimes (x-y direction) and hysteresis of the SWCC compared to the base case.

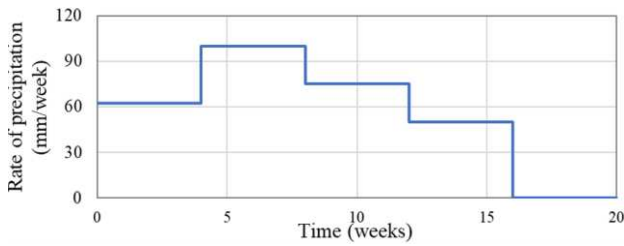


Figure 9. Precipitation input for the analysis.

4 RESULTS

First, the Factor of Safety under dry conditions (water at the foundation level) was computed, obtaining an FoS of 2.65. After this, the base case scenario was computed from week 0 (no precipitation, end of the steady-state analysis) to week 20. Based on this, Figure 10 presents the results of pore water pressures (pwp) at the end of the steady-state analysis and the FoS for that condition (FoS=1.56) for the base case. The light blue dashed lines above the phreatic level (continue blue line) shows how the phreatic surface rises with the precipitation input.

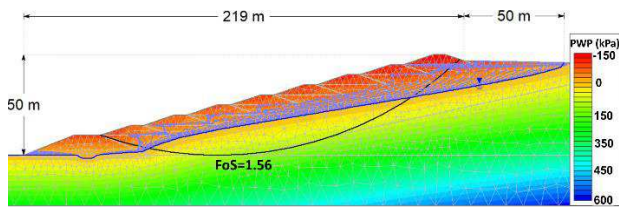


Figure 10. FoS change depending on the drain condition.

To understand the effect of a properly functioning drain, Figure 11 shows the same situation previously shown in Figure 10. However, Figure 11 shows the results considering a clogged drain, where no zero-pressure boundary condition was applied, but still, its permeability of $1 \cdot 10^{-4}$ m/s is considered.

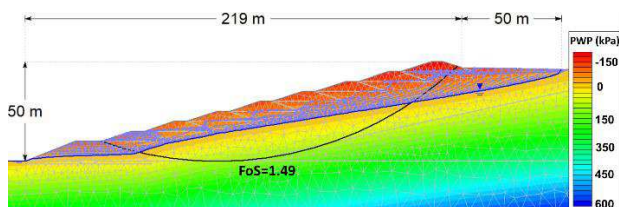


Figure 11. FoS change depending on the drain condition.

From Figure 10 and Figure 11, a clean and properly designed drain considerably reduces the position of the phreatic surface within the dam, especially in the zone close to the dam's toe, where the phreatic surface is expected to rise more. In addition, Figure 10 and Figure 11 show that this effect is not so straightforward after the steady-state condition (dashed lines). This is also reflected in a slight reduction of 5% of the FoS. Consequently, Figure 12 shows the FoS change along the weeks of precipitation and the same case for different beach lengths.

From Figure 12, the significant difference between the drainage condition occurs after week 4, when the significant precipitation rate begins (100 mm/week). In the same way, this influence is maximum by week 20, even considering that after week 16, there is no more precipitation entering the model.

Regarding the influence of the beach length (BL), Figure 12 shows that increasing the BL to 100 and 150 m also increases around 30% and 40% of the FoS during the time, respectively. However, the increase in the FoS stabilises after a BL of 150 m, and the gaining in the FoS becomes less than 5% in time. These results are consistent with Sarsby (2013) findings, who established that ratios of L/H (see Figure 8) around five are undesirable, and more than ten are stable in terms of stability.

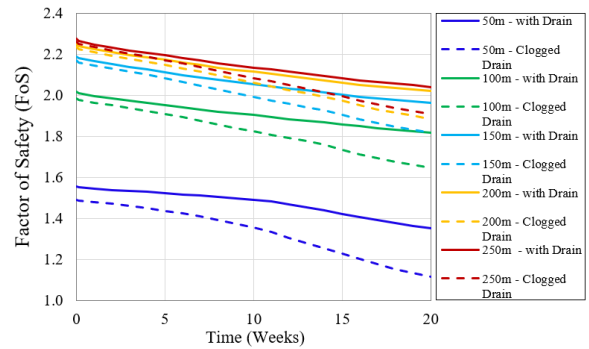


Figure 12. FoS change depending on the drain condition.

Continuing with the analyses, other parameters were assessed independently, such as considering a uniform beach without the transition zone of coarse slimes (i.e. all the slimes are fine slimes), a beach without anisotropy ($k_h = k_v$) and neglecting the hysteresis of the SWCC (i.e. only the drying SWCC path is considered). Figure 13 summarises the change of the FoS in time obtained for each case considering a BL of 50 m.

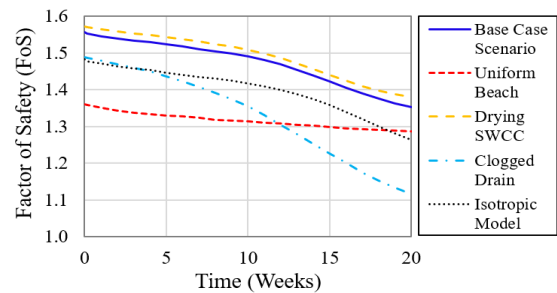


Figure 13. FoS change for each case analysed.

First, from the steady-state analysis, the effect of a uniform fine beach produces a higher phreatic surface compared to the base case scenario, reducing the unsaturated zone, and therefore the suctions and the shear strength in the partially saturated zone. In addition, it is much harder for the precipitation to flow into the unsaturated zone and join the phreatic surface. Therefore, the decrease in the FoS takes more time, and by the end of week #20 of analysis, it reaches just a reduction of 5% compared to the 13% of reduction that the base case scenario experiences in the same time frame.

Regarding the effect of considering an isotropic model with all the horizontal permeability equal to the vertical permeability, the reduction in the FoS is constant and around 5% in time compared to the base case. Considering only the vertical component of permeability, which is lower than the horizontal, it produces a similar effect to a uniform beach, increasing the phreatic surface and reducing the FoS. However, in this case, the transition zone has a higher permeability than the slimes. Hence the reduction in the FoS is constant in time (compared to the base case, see Figure 13).

In terms of the hysteresis of the SWCC, Figure 13 shows that the effect of considering the wetting or drying path of the SWCC affects less than 5% of the obtained results. However, there is an increase in the FoS by considering the drying path of the SWCC. These minor differences can be explained by the fact that the drying path can hold higher suctions for the same water content. Hence, a model that uses an SWCC curve for wetting is slightly more optimistic since it will predict more significant shear strengths.

5 CONCLUSIONS

The factor that most influences the dam's stability regarding the FoS is the pond's position on the impoundment or the beach

length. However, there seems to be a relationship between the height of the TSF and the beach length (L/H), suggesting a specific threshold where the dam could experience some internal instabilities. However, to establish this relationship, several upstream dam geometries (dam heights and beach lengths) should be analysed, incorporating different rainfall conditions and the effect of foundation soil into the flow analysis.

The efficiency and sound design of the drainage system are essential to prevent the phreatic surface from rising at the toe of the dam. The results show that the rising of the phreatic surface in this zone can affect the FoS significantly. In addition, the appearance of water on the face of the tailings sands embankments can cause piping which can severely affect the dam's stability. However, this effect was not analysed in this research.

Hydraulic conductivity anisotropy and lateral variation of the permeability at the impoundment should be incorporated to obtain more realistic results. However, considering this effect leads to a lower phreatic surface within the dam that could be considered a little conservative. Nonetheless, its effect plays a secondary role compared to the factors already mentioned.

On the other hand, the use of the drying or wetting SWCC to represent wetting events has a minimal impact on the phreatic surface and stability.

In terms of the SWCC fitting, Fredlund and Xing (1994) model provide better results than van Genuchten (1980) equation, especially for fine soils. This difference was not significant in sands. In addition, the results suggest that the correction factor of Fredlund & Xing (1994) equation has a lower impact on the fitting.

Finally, it is essential to increase the data regarding shrinkage curves in tailings, otherwise the equivalence between the $w - SWCC$ and the $\theta_w - SWCC$ may be little representative of reality.

6 FUTURE RESEARCH

This study was carried out considering only the drained properties of the soil. However, different authors have shown that failures in TSFs tend to occur under undrained conditions, usually involving sudden strain-softening failures (flow liquefaction type). Future research should follow this research line, considering the undrained behaviour for suctions below the AEV (saturated zone), with constitutive models that can represent the strain-softening of the material. On the other hand, for suctions greater than the ψ_{AEV} , numerical models should incorporate the unsaturated shear strength with a variable ϕ^b according to the matrix suction level.

In terms of the boundary conditions, models should be able to incorporate more than one boundary condition at the same time. Other factors such as the ongoing consolidation in the slimes, raising of the pond level due to rain, and feasibility of overtopping failures due to ponding at the impoundment should also be considered.

7 ACKNOWLEDGEMENTS

This work was funded by the National Agency for Research and Development (ANID) scholarship programme MAGISTER EN AREAS PRIORITARIAS BECAS CHILE/2019 – 730200072 as part of the MSc studies of the main author. In addition, the main author would like to thank SRK Consulting for their support and funding to participate in this conference.

8 REFERENCES

Blight, G. E. (2010). *Geotechnical Engineering for Mine Waste Storage Facilities*. Taylor & Francis.

- Brisson, P. (2006). *Unsaturated flow in tailings*. MSc Dissertation. University of Ottawa.
- Climate-Data.org. (n.d.). BELO HORIZONTE CLIMATE (BRAZIL). Retrieved August 15th, 2020, from BELO HORIZONTE WEATHER BY MONTH // WEATHER AVERAGES: <https://en.climate-data.org/south-america/brazil/minas-gerais/belo-horizonte-2889/#:~:text=In%20Belo%20Horizonte%2C%20the%20average,inch%20of%20precipitation%20falls%20annually>.
- Fredlund, D. G., & Xing, A. (1994). Equations for the soil-water characteristic curve. *Canadian Geotechnical Journal*, 31, 521-532.
- Fredlund, D. G., Rahardjo, H., & Fredlund, M. D. (2012). *Unsaturated Soil Mechanics in Engineering Practice*. New Jersey: John Wiley & Sons.
- Fredlund, D. G., Xing, A., & Huang, S. (1994). Predicting the permeability function for unsaturated soils using the soil-water characteristic curve. *Canadian Geotechnical Journal*, 31, 533-545.
- Fredlund, D.G., & Rahardjo, H. (1993). *Soil mechanics for unsaturated soils*. New York: Wiley.
- Fredlund, D.G., Morgenstern, N. R., & Widger, R. A. (1978). The shear strength of unsaturated soils. *Géotechnique*, 313-321.
- Fredlund, M. D., Wilson, G. W., & Fredlund, D. G. (2002a). Representation and estimation of the shrinkage curve. *Proceeding of the Third International Conference on Unsaturated Soils* (pp. 145-149). Recife, Brazil: UNSAT 2002.
- Heidarian, P. (2012). *Effect of Initial Water Content and Stress History on Water-Retention Behaviour of Mine Tailings*. MSc Dissertation. Carleton University.
- Kulhawey, F. H., & Mayne, P. W. (1990). *Manual on estimating soil properties for foundation design*. Research Report EERI EL-6800. Palo Alto, California: Electric Power Research Institute.
- Leong, E. C., & Rahardjo, H. (1997). Permeability functions for unsaturated soils. *Journal of Geotechnical and Geoenvironmental Engineering*, ASCE, 123, 1118-1126.
- Malaya, C., & Sreedeeep, S. (2012). Critical Review on the Parameters Influencing Soil-Water Characteristic Curve. *Journal of Irrigation and Drainage Engineering*, 138(1), 55-62.
- Morgenstern, N. R., Vick, S. G., & Van Zyl, D. (2015). *Independent Expert Engineering Investigation and Review Panel: Report on Mount Polley Tailings Storage Facility Breach*.
- Morgenstern, N. R., Vick, S. G., Viotti, C. B., & Watts, B. D. (2016). *Fundão Tailings Dam Review Panel: Report on the Immediate Causes of the Failure of the Fundão Dam*.
- Musso, J., & Suazo, G. (2019). Determinación de la curva de retención de agua para relaves multimetálicos de la industria minera de Chile. *Obras y Proyectos*, 25, 22-29.
- O'Gorman, P. A. (2015). Precipitation extreme under climate change. *Current Climate Change Reports*, 49-59.
- Qiu, Y., & Segó, D. C. (2001). Laboratory properties of mine tailings. *Canadian Geotechnical Journal*, 38, 183-190.
- Rico, M., Benito, G., Salgueiro, A. R., Diez-Herrero, A., & Pereira, H. G. (2008). Reported tailings dam failures A review of the European incidents in the worldwide context. *Journal of Hazardous Materials*, 846-852.
- Robertson, P. K., de Melo, L., Williams, J. D., & Wilson, G. W. (2019). *Report of the Expert Panel on the Technical Causes of the Failure of Feijão Dam I*.
- Sarsby, R. W. (2013). Chapter 15: Tailings dams. In R. W. Sarsby, *Environmental Geotechnics* (pp. 365-391). ICE Publishing.
- Spencer, E. (1967). A Method of Analysis of The Stability of Embankments Assuming Parallel Interslice Forces. *Géotechnique* 17, 11-26.
- Valenzuela, L. (2015). *Tailings Dams and Hydraulic Fills – The 2015 Casagrande Lecture*. *Geotechnical Synergy in Buenos Aires 2015*, 5, pp. 5-49.
- van Genuchten, M. T. (1980). A closed-form equation for predicting the hydraulic conductivity of unsaturated soils. *Soil Science Society of America Journal*, 892-898.
- Vick, S. G. (1983). *Planning, Design and Analysis of Tailings Dams*. John Wiley & Sons.
- Zhai, Q., & Rahardjo, H. (2012). Determination of soil-water characteristic curve variables. *Computers and Geotechnics*, 37-43.